

New Types of Nonclassical Iridium Carbonyls Formed in Ir-ZSM-5: A Fourier Transform Infrared Spectroscopy Investigation

M. Mihaylov,[†] E. Ivanova,[†] F. Thibault-Starzyk,[‡] M. Daturi,[‡] L. Dimitrov,[§] and K. Hadjiivanov^{*,†}

Institute of General and Inorganic Chemistry, Bulgarian Academy of Sciences, Sofia 1113, Bulgaria, Laboratoire Catalyse et Spectrochimie, CNRS-ENSICAEN, Université de Caen, 6, bd. Maréchal Juin, 14050 Caen Cedex, France, and Central Laboratory of Mineralogy and Crystallography "Acad. Ivan Kostov", Bulgarian Academy of Sciences, Sofia 1113, Bulgaria

Received: December 7, 2005; In Final Form: March 22, 2006

In this work we report some new nonclassical carbonyls of iridium formed after CO adsorption on Ir-ZSM-5 (Ir-MFI). Mainly Ir⁺ cations were found on sample activated at 523 K and reduced by CO at the same temperature. With CO they formed Ir⁺(CO)₂ gem-dicarbonyls (2104 and 2033 cm⁻¹) that decomposed at 673 K without leaving a measurable fraction of monocarbonyls. The dicarbonyl structure was established by ¹²CO–¹³CO coadsorption experiments. In the presence of CO in the gaseous phase and at ambient temperature the Ir⁺(CO)₂ dicarbonyls were converted into Ir⁺(CO)₃ species (2182, 2099, and 2074 cm⁻¹). At 100 K these complexes are able to accommodate a fourth CO molecule thus producing tetracarbonyls (2155, 2145, 2125, and 2105 cm⁻¹). The results are explained by the high coordinative unsaturation of the Ir⁺ cations in the ZSM-5 matrix. This is also the reason for the formation of mixed Ir⁺(H₂O)(CO)₂ species after CO–H₂O coadsorption (2087 and 2015 cm⁻¹). Evacuation of the sample at 673 K, followed by treatment with CO at 523 K, generates Ir²⁺ cations. With CO these cations form another kind of geminal complex, namely, Ir²⁺-(CO)₂ species (2173 and 2129 cm⁻¹). Here again, the structure was confirmed by ¹²CO–¹³CO coadsorption experiments. These dicarbonyls are decomposed at 573 K (again without producing monocarbonyls) and are able to accommodate additionally neither CO nor water molecules. The results are explained by the smaller cationic radius of Ir²⁺ (as compared to Ir⁺), which is associated with a decrease of the number of ligands required for coordinative saturation.

1. Introduction

The so-called nonclassical carbonyls are formed when CO is coordinated to metal cations instead of neutral atoms.^{1,2} An important peculiarity of these compounds is that the σ -bond is rather important, in contrast to the classical metal carbonyls. On the basis of its ability to form surface complexes with both metallic and cationic sites and the sensitivity of the C–O stretching modes to the nature of the M–CO bond formed, CO is the most used IR probe molecule for testing catalyst surfaces.^{3–5} The increase in oxidation state of the cation leads to enhancement of the metal–CO bond σ -component and of the electrostatic interaction, which results in an increase of the CO stretching frequency.

The cations in zeolites are characterized by high coordinative unsaturation and high electrophilicity. Consequently, in many cases they can adsorb two,^{6,7} three,^{8–12} and even four CO molecules simultaneously.^{13–15} Thus, zeolites are suitable matrixes for the isolation of polycarbonyl species. However, for steric reasons, the symmetry of these carbonyls differs from the symmetry of matrix-isolated species, which makes the analogy in their spectral performances difficult.

Although iridium is not widely used in catalysis due to its high cost and rarity, it is promising for some reactions. Thus, it has recently been reported that supported iridium was very efficient in NO reduction, CO oxidation,¹⁶ and the catalytic CO₂ reforming of methane.¹⁷ Many authors attribute this catalytic activity to the presence of cationic iridium or to the coexistence of metal and oxide phases.^{16,18} That is why a detailed characterization of iridium in different oxidation states is of particular importance.

The aim of this study is to investigate CO adsorption on an Ir-ZSM-5 (Ir-MFI) sample. We expect that iridium cations in the ZSM-5 matrix should be low-coordinated and thus able to adsorb more than one CO molecule. Both the properties of iridium itself and the high coordinative unsaturation of the Irⁿ⁺ cations could be important in catalysis.

The data on CO adsorption of Ir-containing samples are scarce. Solymosi et al.¹⁹ studied a reduced Ir/Al₂O₃ sample. After CO adsorption, the authors observed a weak band at 2080–2050 cm⁻¹, which they attributed to Ir⁰–CO species and a set of two bands at 2107–2090 and 2040–2010 cm⁻¹, which were assigned to the symmetric and antisymmetric modes, respectively, of Ir⁺(CO)₂ dicarbonyls. When the adsorption was initially performed at low temperature, only an Ir⁰–CO band was detected. With the increase of temperature, the Ir⁺(CO)₂ bands developed, this was attributed to CO-induced oxidation of metallic iridium by the surface OH groups of the support. Lefebvre et al.²⁰ reported the conversion of Ir⁺(CO)₂ into Ir⁺-(CO)₃ species (2115–2100 and 2087–2080 cm⁻¹) in different

* Author to whom correspondence should be addressed. Phone: 003592 9793598. Fax: 003592 8705024. E-mail: kih@svr.igic.bas.bg.

[†] Institute of General and Inorganic Chemistry, Bulgarian Academy of Sciences.

[‡] Université de Caen.

[§] Central Laboratory of Mineralogy and Crystallography "Acad. Ivan Kostov", Bulgarian Academy of Sciences.

iridium-containing zeolites (Ir/NaFAU, Ir/LaFAU, Ir/NaMOR) but provided no details on the spectral behavior of the dicarbonyl species. Gelin et al.²¹ investigated an Ir/NaFAU sample prepared using an Ir³⁺ precursor. Upon CO adsorption they observed a band at 2100 cm⁻¹ and attributed it to Ir³⁺-CO species. In the presence of CO at 443 K they detected new bands at 2102–2086 and 2030–2001 cm⁻¹.²¹ On the basis of volumetric measurements (showing a high CO-to-Ir ratio) and isotopic exchange studies, these bands were assigned to Ir⁺(CO)₃ species. However, more recently the same authors²² reassigned the set of bands to Ir⁺(CO)₂ dicarbonyls. They also distinguished two types of these species: a set of bands at 2088 and 2003 cm⁻¹ and a set of bands at 2102 and 2020 cm⁻¹, depending on the presence of water on the sample. Bukhardt et al.²³ also observed Ir⁺(CO)₂ species on their Ir/DAY (dealuminated FAU) sample (bands at 2108 and 2037 cm⁻¹). The dicarbonyl structure was unambiguously established by means of ¹²CO–¹³CO coadsorption. They observed no CO adsorption on an oxidized sample (Ir³⁺-DAY) and detected the dicarbonyl species only after reduction of the sample with CO.²³ The remarkable analogy between the carbonyls of iridium and rhodium is worth noting. It is well established that Rh⁺(CO)₂ species are generally observed after CO adsorption on Rh-containing samples.^{3,13,14,24,25} No corresponding linear monocarbonyl species are typical; i.e., the dicarbonyls are *complex-specified*.²⁶ The same seems to be true for Ir⁺(CO)₂.

2. Experimental Section

The Ir-ZSM-5 sample was prepared by solid-state ion exchange. The starting H-ZSM-5 material was supplied by Degussa (Si/Al = 26.8). First, 1.00 g of the zeolite (dried at 623 K for 4 h) was mechanically mixed with 0.10 g of IrCl₃·3H₂O (Johnson Matthey). Preliminary experiments have shown that the exchange procedure is effective using this water-soluble (dark-green) form instead of the nonsoluble red IrCl₃. The iridium precursor used contained 53.80 wt % Ir. Several drops of distilled water were added to the mixture of the zeolite and IrCl₃·3H₂O until a consistent cake was formed. The cake was homogenized with a Teflon spatula, dried at 373 K for 5 h in an oven, and then transferred to a quartz reactor. To perform solid-state ion exchange, the dried sample was heated in a flux of dry Ar (40 mL min⁻¹) at 723 K for 5 h. The temperature was reached by a temperature ramp of 2 K min⁻¹. Then it was thoroughly washed with deionized water until a negative reaction for chlorine anions. The iridium concentration in the sample was 4.92 wt % Ir.

The IR spectra were recorded on a Bruker S 66 spectrometer equipped with a mercury cadmium telluride (MCT) detector at a spectral resolution of 4 cm⁻¹, accumulating 128 scans. Self-supporting pellets (ca. 10 mg cm⁻²) were prepared from the sample powder and treated directly in the purpose-made IR cell. The latter was connected to a vacuum-adsorption apparatus with a residual pressure below 10⁻³ Pa. Prior to the adsorption measurements, the samples were activated by prolonged (1 night) evacuation at room temperature and 1 h evacuation at 523 K (temperature ramp of 2 K min⁻¹). Then the sample was reduced with CO (5.3 kPa) for 1 h at 523 K and evacuated at the same temperature. Later we shall refer to this procedure as activation procedure 1. Activation procedure 2 is the same except that adsorbed CO was evacuated at 673 K for 15 min, followed by additional CO reduction at 523 K.

Carbon monoxide (> 99.997%) was supplied by Air Liquide, France. Labeled carbon monoxide (¹³C isotopic purity of 92.9 at. %) was delivered by CEA-ORES, France. Before use, carbon monoxide was passed through a liquid nitrogen trap.

Iridium concentration in the sample was measured by inductively coupled plasma atomic emission spectroscopy (ICP-AES) with a Longjumeau (France) equipment.

3. Results

3.1. Initial Characterization of the Samples. Preliminary experiments had shown that after evacuation at 673 K for 1 h the sample became black and almost opaque. This may be explained by the autoreduction of iridium and the formation of relatively big metallic particles. Indeed, as reported in the literature,²⁷ the activation procedure for iridium-containing catalysts is decisive for the genesis of supported iridium species. That is why we performed a more gentle treatment before the adsorption experiments (slow heating to 523 K during evacuation), as was mentioned in the Experimental Section.

The IR spectrum of the sample evacuated at 523 K contains, in the OH region, three bands with maxima at 3744, 3665 (vw), and 3610 cm⁻¹. The band at 3744 cm⁻¹ is due to silanol groups, and the 3610 cm⁻¹ band to the acidic zeolite Si–OH–Al hydroxyls. The latter band had a lower intensity than in the case of H-ZSM-5, which implied some exchange of protons with iridium cations. The weak band at 3665 cm⁻¹ has occasionally been seen for the H-ZSM-5 and M-ZSM-5 zeolites and was assigned to small amounts of water adsorbed on the Brønsted acid sites²⁸ or to Al–OH species. However, we cannot totally rule out the possibility that this band represents surface Irⁿ⁺–OH groups.

The adsorption of CO on the sample evacuated at 523 K led to the appearance of a series of very weak bands in the carbonyl stretching region, their maxima being at 2127, 2100, 2070, 2033, and 2011 cm⁻¹. Because these bands were much more pronounced with the CO-reduced sample, they will be discussed later.

The background spectrum of the sample remained practically the same after reduction with CO at 523 K, followed by evacuation at the same temperature (activation procedure 1). Only four bands are left in the carbonyl stretching region, their maxima being at 2127, 2104, 2033, and 2011 cm⁻¹. These bands are due to stable carbonyls species and will be discussed in what follows. All bands disappeared after evacuation for 15 min. at 673 K.

3.2. Adsorption of CO at Ambient Temperature on Ir-ZSM-5. After adsorption of CO (400 kPa equilibrium pressure) on the Ir-ZSM-5 sample (activated by procedure 1), a series of bands in the carbonyl stretching region were registered: 2182-(w), 2147(w), 2127(sh), 2099(s), 2074(s), 2033(s), and 2011-(sh) cm⁻¹ (Figure 1, spectrum a). Decrease of the equilibrium pressure and evacuation (Figure 1, spectra b–d) provoked a decrease in intensity and disappearance of the bands at 2182, 2147, 2099, and 2074 cm⁻¹. On the contrary, the band at 2033 cm⁻¹ developed and a new band at 2104 cm⁻¹ (initially masked by the 2099 cm⁻¹ band) emerged. Difference spectra revealed that the shoulders at 2127 and 2111 cm⁻¹ were hardly affected. A very weak band at 2159 cm⁻¹ and a weak one around 2070 cm⁻¹ became also observable.

Evacuation at elevated temperatures led to a fast disappearance of the bands at 2159 and 2070 cm⁻¹ (Figure 2, spectrum b). The two bands at 2104 and 2033 cm⁻¹ decreased in concert (Figure 1, spectra b–d). The shoulders at 2127 and 2111 cm⁻¹ also decreased in synchrony, somewhat faster than the principal bands at 2104 and 2033 cm⁻¹. All bands practically disappeared after evacuation at 673 K (Figure 2, spectrum e).

Taking into account the behavior of the bands at 2104 and 2033 cm⁻¹ and in agreement with literature data,^{19,22,23} we

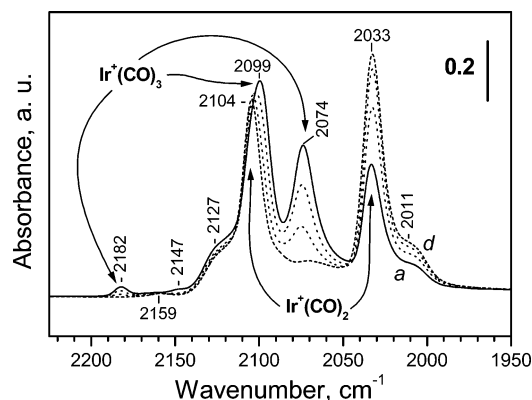


Figure 1. Fourier transform infrared spectra of CO adsorbed on Ir-ZSM-5. Equilibrium CO pressure of 400 Pa (a) and evolution of the spectra under dynamic vacuum (b–d). The spectra are corrected by background subtraction.

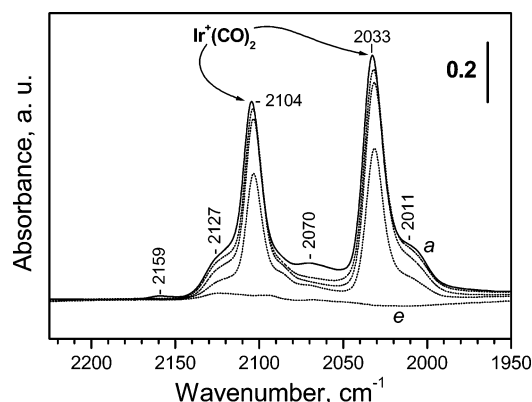


Figure 2. Fourier transform infrared spectra of CO adsorbed on Ir-ZSM-5. Adsorption of CO (400 Pa) at ambient temperature followed by 10 min evacuations at ambient temperature (a) and at 523 (b), 573 (c), 623 (d), and 673 K (e). The spectra are corrected by background subtraction.

assigned them to the symmetric and antisymmetric modes, respectively, of $\text{Ir}^+(\text{CO})_2$ species. For convenience, the assignments of all carbonyl bands observed in this study are summarized in Table 1.

Careful analysis of the spectra presented in Figure 1 indicates that the $\text{Ir}^+(\text{CO})_2$ bands at 2104 and 2133 cm^{-1} develop with decreasing coverage, at the expense of the bands at 2182, 2099, and 2074 cm^{-1} . This indicates that under CO pressure the $\text{Ir}^+(\text{CO})_2$ species accept an additional CO molecule and form tricarbonyls. The appearance of three IR bands for these species indicates a symmetry lower than C_{3v} . Since the band at 2182 cm^{-1} appeared with a very low intensity, we can stress that the C_{3v} symmetry is slightly distorted. A similar conversion has been reported for Rh-ZSM-5; in that case the $\text{Rh}^+(\text{CO})_2$ species

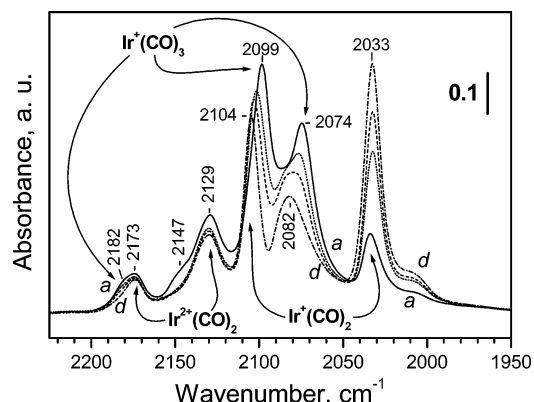


Figure 3. Fourier transform infrared spectra of CO adsorbed on Ir-ZSM-5 after second reduction. Equilibrium CO pressure of 5.3 kPa CO (a) and evolution of the spectra under dynamic vacuum (b–d). The spectra are corrected by background subtraction.

(2114 and 2048 cm^{-1}) have also been converted into tricarbonyls (2181, 2118, and 2084 cm^{-1}) in the presence of CO.¹⁴

The band at 2159 cm^{-1} is easily removed by evacuation at 373 K and probably characterizes carbonyls of Ir^{2+} ions. The band at 2147 cm^{-1} will be assigned below.

After evacuation of the sample at 673 K, it was again reduced with CO at 523 K and evacuated at the same temperature (activation procedure 2). New carbonyl bands at 2173 and 2129 cm^{-1} were detected, and the bands at 2127, 2104, 2033, and 2011 cm^{-1} were observed with reduced intensity. Then CO (5.3 kPa) was added into the cell. The bands at 2173 and 2129 cm^{-1} were not affected (Figure 3, spectrum a). These two bands were stable toward evacuation at ambient temperature (Figure 3, spectra b–d) and disappeared after evacuation at 573 K (spectra not shown). They changed in concert, which implied that they characterized one kind of species. The ^{12}CO – ^{13}CO coadsorption experiments (see below) proved their dicarbonyl structure. The higher frequency of the respective bands, as compared to the bands due to $\text{Ir}^+(\text{CO})_2$ species, presupposed an oxidation state of the complexing iridium cation higher than one. In this case one should expect a more restricted π -back-donation and, consequently, a lower stability of the dicarbonyls. Indeed, these species were found to be less stable than the $\text{Ir}^+(\text{CO})_2$ species. On the basis of these considerations, we assigned the bands at 2173 and 2129 cm^{-1} to the ν_s and ν_{as} , respectively, of Ir^{2+} – $(\text{CO})_2$ species. Similar dicarbonyls (2176 and 2142 cm^{-1}) with the participation of Rh^{2+} cations were recently reported with a Rh-ZSM-5 sample.²⁴

As in the previous case, evacuation led to conversion of $\text{Ir}^+(\text{CO})_3$ (2182, 2099, and 2074 cm^{-1}) into $\text{Ir}^+(\text{CO})_2$ (2104 and 2033 cm^{-1}) species (Figure 3, spectra b–d). A new, relatively intense band at 2082 cm^{-1} was demasked at low coverages (Figure 3, spectra c and d). This band was progressively blue-

TABLE 1: Assignment of the Infrared Carbonyl Bands Observed in This Study

species	bands	comments
$\text{Ir}^+(\text{CO})_2$	2104 and 2033 cm^{-1}	Decomposed without producing monocarbonyls (complex-specified species); stable to ca. 673 K; able to accommodate stepwise two more CO molecules.
$\text{Ir}^+(\text{H}_2\text{O})(\text{CO})_2$	2087 and 2015 cm^{-1}	The H_2O ligand is lost by evacuation at ambient temperature.
$\text{Ir}^+(\text{CO})_3$	2182 (w), 2099, and 2074 cm^{-1}	Formed at ambient temperature under CO.
$\text{Ir}^+(\text{CO})_4$	2155, 2145, 2125, and 2105 cm^{-1}	Formed at low temperature.
$\text{Ir}^+(\text{CO})_2$	2127 and 2011 cm^{-1}	Decomposed without producing monocarbonyls (complex-specified species); stable to ca. 673 K; not able to accommodate additional CO molecules. The Ir^+ cations are probably not in exchange positions.
$\text{Ir}^{2+}(\text{CO})_2$	2173 and 2129 cm^{-1}	Complex-specified species. Stable to ca. 573 K.
Ir^{2+} –CO	2159 cm^{-1}	Tentative assignment. Ir^{2+} probably not in cationic positions.
Ir^0 –CO	2082–2060 cm^{-1}	Stable to $T < 573$ K; the band maximum red shifted with coverage increase.
OH–CO	2175 cm^{-1}	Formed at low temperature.

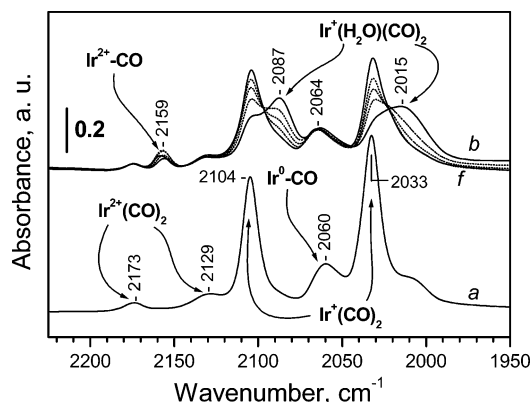


Figure 4. Fourier transform infrared spectra of CO and H₂O co-adsorbed on Ir-ZSM-5. Adsorption of CO, followed by 5 min evacuation at 473 K (a), subsequent introduction of water vapor (160 Pa equilibrium pressure) (b), and evolution of the spectra under dynamic vacuum (c–f). The spectra are corrected by background subtraction.

shifted with the coverage decrease, down to ca. 2060 cm^{−1} (Figure 4, spectrum a). Such a shift is typical of CO adsorbed on metals. Taking this into account and in agreement with literature data,^{19,29} we assigned the 2082–2060 cm^{−1} band to Ir⁰–CO species, the metallic iridium most probably being produced via reduction by CO during its desorption at high temperatures.

3.3. Coadsorption of CO and H₂O. After 5 min evacuation of CO at 473 K (Figure 4, spectrum a), water vapor (160 Pa) was introduced into the cell. As a result, new bands at 2159, 2087, and 2015 cm^{−1} emerged (Figure 4, spectrum b). The Ir⁺–(CO)₂ bands at 2104 and 2033 cm^{−1} strongly decreased in intensity, and the band at 2060 cm^{−1} was shifted to 2064 cm^{−1}. The bands at 2173 and 2129 cm^{−1} remained practically unaffected. Subsequent evacuation at room temperature provoked a gradual disappearance of the bands at 2087 and 2015 cm^{−1} and the development of the initially registered Ir⁺–(CO)₂ bands at 2104 and 2033 cm^{−1}. These results clearly show that a water molecule can be inserted into the Ir⁺–(CO)₂ species (2104 and 2033 cm^{−1}) forming thus aqua–dicarbonyl complexes (2087 and 2015 cm^{−1}). Evidently, this insertion leads to a rearrangement of the electron density in the complex. Note that no water molecule can be inserted in Ir²⁺–(CO)₂ species.

The decrease in the C–O stretching frequencies of the Ir⁺–(CO)₂ species after insertion of a water molecule in the complex can be explained in two ways:³⁰ (i) increase of the π -component of the Ir⁺–CO bond (water supplying electron density) or decrease of its σ -component because of the decrease in electrophilicity of the Ir⁺ cation caused by the filling of the Ir⁺ coordination sphere by water. We infer that the latter phenomenon prevails. Indeed, an enhanced π -back-donation should lead to an increase in the extinction coefficient,³ while detailed analysis of the spectra showed that it was hardly affected. In addition, a strengthened π -back-donation should lead to strengthening of the Ir⁺–CO bond. However, the total concentration of the Ir⁺–(CO)₂ species had decreased after the experiments, which indicated that the Ir⁺–CO bond had been weakened.

At present we cannot offer an unambiguous assignment of the band at 2159 cm^{−1}. Separate experiments have shown that this band can also be formed in the absence of water, usually during desorption procedures. Since Ir³⁺ cations are believed to form no carbonyl species,²³ we tentatively assign the band at 2159 cm^{−1} to Ir²⁺–CO monocarbonyls, as proposed above. Indeed, the C–O frequency of these species is observed between the symmetric and antisymmetric modes of the Ir²⁺–(CO)₂ dicarbonyls.

TABLE 2: Angle between the CO Ligands in the Iridium Dicarbonyl Species

species	bands	angle
Ir ⁺ –(CO) ₂	2105 and 2033 cm ^{−1}	95°
Ir ⁺ –(H ₂ O)–(CO) ₂	2087 and 2015 cm ^{−1}	82°
Ir ²⁺ –(CO) ₂	2173 and 2129 cm ^{−1}	ca. 100° ^a

^a This calculation is imprecise because of the superimposition of bands.

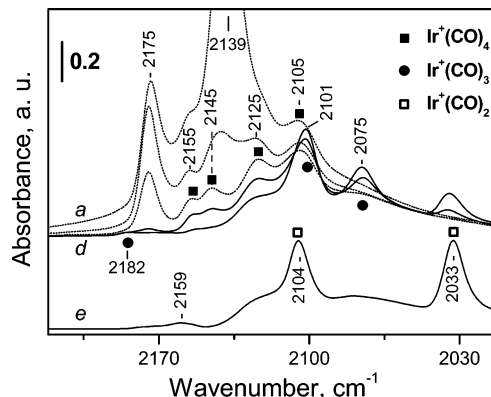


Figure 5. Fourier transform infrared spectra of CO adsorbed on Ir-ZSM-5 at 100 K. Equilibrium CO pressure of 220 Pa (a) and evolution of the spectra under dynamic vacuum at 100 K (b–d) and ambient temperature (e). The spectra are corrected by background subtraction.

It is well-known that the ratio between the integral intensities of the ν_{as} and ν_s C–O modes in the geminal dicarbonyls depends on the angle (Θ) between the two CO molecules³¹

$$I_{\text{asym}}/I_{\text{sym}} = \tan^2(\Theta/2) \quad (1)$$

Using eq 1, we calculated the angles between the CO ligands in the different dicarbonyls (Table 2). The angle for the Ir⁺–(CO)₂ species was 95°, while in the Ir⁺–(H₂O)–(CO)₂ complexes, it was 82°. Indeed, it is normal to expect that the increase in the number of the ligands will lead to a decrease of the angle between them.

3.4. Adsorption of CO at Low Temperature. To check the possibility of additional CO molecules to be coordinated to the iridium cations in the polycarbonyl species, namely, Ir⁺–(CO)₃ and Ir²⁺–(CO)₂, we studied CO adsorption at ca. 100 K. Introduction of CO (200 Pa, ca. 100 K) to the cell provoked the appearance of four principal bands in the carbonyl region, namely, at 2175, 2155, 2139, and 2105 cm^{−1} (Figure 5, spectrum a). Evacuation at 100 K resulted in a fast decrease in intensity of the 2139 cm^{−1} band, which led to demasking of two bands at 2145 and 2125 cm^{−1} (Figure 5, spectrum b). Further evacuation led to a decrease in intensity and disappearance of the bands at 2175, 2155, 2145, 2125, and 2105 cm^{−1} (Figure 5, spectra c–e). Bands due to Ir⁺–(CO)₃ species (2182, 2101, and 2075 cm^{−1}) started to develop (Figure 5, spectra d and e), followed by the characteristic band of Ir⁺–(CO)₂ at 2033 cm^{−1}. (The band at 2105 cm^{−1} was masked by the band at 2101 cm^{−1}.)

The band at 2139 cm^{−1} is usually detected after low-temperature CO adsorption on zeolites and characterizes physically adsorbed CO. The band at 2175 cm^{−1} changed in synchrony with a 315 cm^{−1} red shift of the OH band at 3610 cm^{−1} and is, therefore, assigned to OH–CO species.

The development of the tricarbonyl bands with decreasing coverages implies that these species are produced by destruction of another species, namely, tetracarbonyls. Analysis of the spectra shows that the Ir⁺–(CO)₄ complexes are characterized by a set of bands at 2155, 2145, 2125, and 2105 cm^{−1}. Note

TABLE 3: Observed and Calculated Frequencies of the Infrared Carbonyl Bands of Iridium Polycarbonyls after Substitution of ^{12}CO by ^{13}CO

species	observed bands	calculated frequencies
$\text{Ir}^+(\text{}^{12}\text{CO})_2$	2104 and 2033 cm^{-1}	
$\text{Ir}^+(\text{}^{12}\text{CO})(\text{}^{13}\text{CO})$	2088 and 2002 cm^{-1}	2088 and 2004 cm^{-1}
$\text{Ir}^+(\text{}^{13}\text{CO})_2$	2055 and 1986 cm^{-1}	2058 and 1988 cm^{-1}
$\text{Ir}^+(\text{}^{12}\text{CO})_3$	2182 (w), 2099, and 2075 cm^{-1}	
$\text{Ir}^+(\text{}^{12}\text{CO})_2(\text{}^{13}\text{CO})$	2078 and 2032 cm^{-1}	
$\text{Ir}^+(\text{}^{12}\text{CO})(\text{}^{13}\text{CO})_2$	2069 and 2029 cm^{-1}	
$\text{Ir}^+(\text{}^{13}\text{CO})_3$	2053 and 2026 cm^{-1}	2133, 2053, and 2027 cm^{-1}
$\text{Ir}^{2+}(\text{}^{12}\text{CO})_2$	2172 and 2128 cm^{-1}	
$\text{Ir}^{2+}(\text{}^{12}\text{CO})(\text{}^{13}\text{CO})$	2157 and 2090 cm^{-1}	2158 and 2093 cm^{-1}
$\text{Ir}^{2+}(\text{}^{13}\text{CO})_2$	ca. 2120 and 2078 cm^{-1}	2123 and 2081 cm^{-1}

that one of these bands (2105 cm^{-1}) coincides with the ν_s mode of the $\text{Ir}^+(\text{CO})_2$ species.

3.5. ^{12}CO – ^{13}CO Coadsorption Experiments. To prove the structure of the two kinds of dicarbonyl species observed in this work, we studied the coadsorption of ^{12}CO and ^{13}CO . If the respective species were dicarbonyls, then four new bands for each of them should have been observed after ^{12}CO – ^{13}CO coadsorption: (i) two bands due to the symmetric and antisymmetric modes of the $\text{Ir}^{n+}(\text{}^{13}\text{CO})_2$ species, respectively, and (ii) two bands arising from mixed-ligand species, $\text{Ir}^{n+}(\text{}^{12}\text{CO})(\text{}^{13}\text{CO})$, namely, $\nu(\text{}^{12}\text{CO})$ and $\nu(\text{}^{13}\text{CO})$. Using an approximate force-field model,³¹ we calculated the frequencies of the complexes containing one or two ^{13}CO molecules. The results are presented in Table 3.

A new pellet was subjected to activation procedure 1, and CO was adsorbed on it. After evacuation of CO the already described bands at 2127, 2104, 2033, and 2011 cm^{-1} were registered (Figure 6, spectrum a). Then some amount of ^{13}CO (ca. 0.8 μmol) was added to the cell and evacuated (evacuation was performed to destruct the tricarbonyl species). As a result, the $\text{Ir}^+(\text{}^{12}\text{CO})_2$ bands at 2104 and 2033 cm^{-1} decreased in intensity, and four new bands, at 2088, 2055, 2002, and 1986 cm^{-1} , emerged. Comparison with the calculated values presented in Table 3 allows us to assign unambiguously (i) the bands at 2055 and 1986 cm^{-1} to the ν_s and ν_{as} , respectively, of $\text{Ir}^+(\text{}^{13}\text{CO})_2$ species, and (ii) the bands at 2088 and 2002 cm^{-1} , to the $\nu(\text{}^{12}\text{C}=\text{O})$ and $\nu(\text{}^{13}\text{C}=\text{O})$ modes, respectively, of $\text{Ir}^+(\text{}^{12}\text{CO})(\text{}^{13}\text{CO})$ complexes. Hence, the experiments with labeled CO clearly demonstrate that the bands at 2104 and 2033 cm^{-1} arise from dicarbonyl species. Note that the shoulders at 2127 and 2111 cm^{-1} were not affected by the addition of ^{13}CO . Hence, the corresponding dicarbonyl species resist isotopic exchange. This is consistent with the observation they are stable at ambient temperature and not able to accommodate additional CO molecules as found in the previous experiments.

Although the frequencies of tricarbonyls with different numbers of ^{12}CO and ^{13}CO ligands are difficult to predict, some experiments were carried out to obtain experimental data on their spectral performance. Analysis of the results (spectra not shown) indicated that the $\text{Ir}^+(\text{}^{12}\text{CO})_2(\text{}^{13}\text{CO})$ species were characterized by bands at 2078 and 2032 cm^{-1} , and the $\text{Ir}^+(\text{}^{12}\text{CO})(\text{}^{13}\text{CO})_2$ species by bands at 2069 and 2029 cm^{-1} .

Another set of experiments was designed to prove the dicarbonyl structure of the $\text{Ir}^{2+}(\text{CO})_2$ dicarbonyls (bands at 2173 and 2129 cm^{-1}). As already established, coordinatively unsaturated (cus) Ir^{2+} cations are created by activation procedure 2. Indeed, bands of the $\text{Ir}^{2+}(\text{CO})_2$ species (2172 and 2128 cm^{-1}) as well as of $\text{Ir}^+(\text{CO})_2$ (2105 and 2033 cm^{-1}) and of $\text{Ir}^0\text{--CO}$ (2052 cm^{-1}) were registered after adsorption of CO followed by evacuation (Figure 7, spectrum a). Subsequent introduction of a ^{12}CO – ^{13}CO isotopic mixture (ca. 500 Pa, ca. 1:1 molar

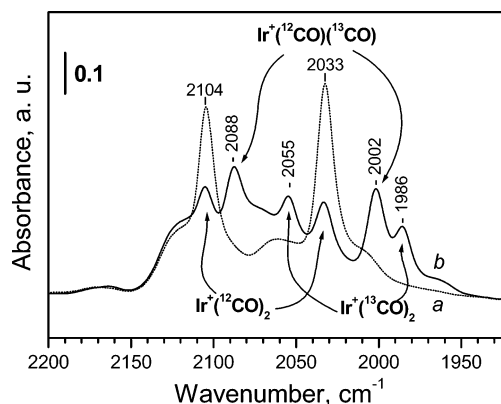


Figure 6. Fourier transform infrared spectra of ^{12}CO and ^{13}CO coadsorbed on Ir-ZSM-5. Sample subjected to activation procedure 1 (a), after introduction of ^{13}CO (ca. 0.8 μmol) and evacuation at ambient temperature (b). The spectra are corrected by background subtraction.

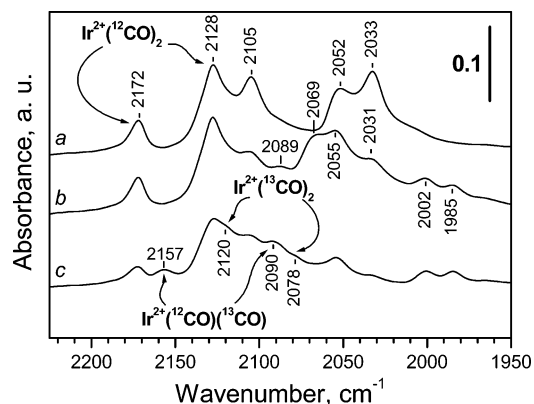


Figure 7. Fourier transform infrared spectra of ^{12}CO and ^{13}CO coadsorbed on Ir-ZSM-5. Sample subjected to activation procedure 2 (a), after introduction of the isotopic mixture ^{12}CO – ^{13}CO (ca. 1:1, 600 Pa equilibrium pressure) (b), and heating of the system at 473 K for 10 min (c). The spectra are corrected by background subtraction.

ratio) resulted in the appearance of the bands due to $\text{Ir}^+(\text{}^{13}\text{CO})_2$ (2055 and 1985 cm^{-1}) and $\text{Ir}^+(\text{}^{12}\text{CO})(\text{}^{13}\text{CO})$ (2089 and 2002 cm^{-1}) species (Figure 7, spectrum b). In addition a band assigned to $\text{Ir}^+(\text{}^{12}\text{CO})(\text{}^{13}\text{CO})_2$ was registered at 2069 cm^{-1} . The bands of the $\text{Ir}^{2+}(\text{CO})_2$ species were not affected. As discussed above, this is due to the fact that these species are (i) stable and (ii) not able to accommodate an additional CO molecule, thus being resistant to exchange of the CO ligands. To ensure some exchange, we heated the sample for 10 min at 473 K in the atmosphere of the isotopic mixture. As a result, the bands at 2172 and 2128 cm^{-1} decreased in intensity and new bands at 2157, ca. 2120, 2090, and 2078 cm^{-1} appeared (Figure 7, spectrum c). Comparison with the calculated values presented in Table 2 allows us to assign the bands at 2157 and 2090 cm^{-1} to $\text{Ir}^{2+}(\text{}^{12}\text{CO})(\text{}^{13}\text{CO})$ species and the bands at ca. 2120 and 2078 cm^{-1} to $\text{Ir}^{2+}(\text{}^{13}\text{CO})_2$ complexes. Hence, in this case again, the dicarbonyl structure was proven by the ^{12}CO – ^{13}CO coadsorption experiments.

4. Discussion

The most typical oxidation states of iridium are 3 and 4, but compounds of Ir^+ , Ir^{2+} , and Ir^{6+} are also known.³² The Ir^{6+} species are unstable and will not be considered here. Ir^+ cations are stabilized in carbonyl complexes.

It was found that adsorption of CO on the nonreduced sample was negligible. This could be explained by the high oxidation state of iridium. Since we used an Ir^{3+} precursor and did not

submit the sample to oxidation pretreatment, we can infer that in the nonreduced Ir-ZSM-5 iridium is encountered as Ir^{3+} cations. These results are consistent with the earlier observation of Bukhardt et al.²³ who have reported that Ir^{3+} cations in Ir/DAY are not able to form carbonyl complexes. Indeed, many cations in a high oxidation state are coordinatively saturated and do not form bonds with CO. This is the case of Mo^{6+} , Cr^{6+} , V^{5+} , and even Fe^{3+} .^{3–5} Note, however, that we cannot totally rule out the possible presence of some Ir^{4+} cations in the nonreduced samples.

On the basis of the chemical composition of the sample, we calculated the Ir/Al molar ratio to be 45.6:100. Formally, if we postulate that one Ir^{3+} cation exchanges three protons, then this ratio corresponds to an exchange degree of 137%. However, it is believed that cations in ZSM-5 can be located in the vicinity of one or two aluminum atoms, respectively.³³ Hence, the exchange degree should be between 45.6% (if all iridium ions are located in vicinity of one aluminum) and 91.2% (in case all iridium ions compensate two charge defects). The real value is rather lower, since some of iridium has most probably another location, as proved by the heterogeneity of iridium revealed by CO adsorption.

4.1. Carbonyl Complexes of Ir^+ in Ir-ZSM-5. It is now well established that many univalent cations cannot be produced by reduction of M^{n+} ($n > 1$) with hydrogen but are created after interaction with CO. Thus, Ni^+ ,⁹ Co^+ ,¹⁵ Pt^+ ,¹⁰ and Rh^+ ^{13,14} cations have been isolated after reduction of the respective samples with CO. This phenomenon is believed to be due to the fact that the $1+$ oxidation state of these cations is stabilized in the carbonyl complexes.

Reduction of our sample with CO also resulted in formation of Ir^+ cations. Testing these cations with CO revealed them to be of two types. The first type of Ir^+ cations formed with CO dicarbonyls (bands at 2104 and 2033 cm^{-1}), tricarbonyls (2182, 2099, and 2074 cm^{-1}), and at low temperature even tetracarbonyls (2155, 2145, 2125, and 2105 cm^{-1}) (Figure 5). Some of the latter species were formed, in the presence of CO, even at ambient temperature, as shown by the band at 2147 cm^{-1} (Figures 1 and 2, spectra a). The second type of Ir^+ cations formed with CO-only dicarbonyls (bands at 2104 and 2033 cm^{-1}) and thus appeared to be more coordinatively saturated.

Tetracarbonyl species are rarely produced after CO adsorption on cationic sites. The only examples known so far are Rh^+ and Co^+ cations in zeolites.^{13–15} In these cases it is considered that the cations are in exchanged positions and low-coordinated, thus being able to adsorb four CO molecules simultaneously. Note, however, that the conversion of the tri- into the tetracarbonyl species is not complete with Co^+ -ZSM-5 and Rh^+ -ZSM-5 even at 100 K. Here, a full conversion to tetracarbonyls is observed, as shown by the absence of the characteristic $\text{Ir}^+(\text{CO})_3$ band at 2075 cm^{-1} (Figure 5, spectrum a). This phenomenon can be explained by the large cationic radius of Ir^+ permitting the formation of the complex without steric hindrance.

It was also found that the dicarbonyl species decompose without producing monocarbonyls. The same is the situation with the well-known $\text{Rh}^+(\text{CO})_2$ gem-dicarbonyls and the $\text{Co}^+(\text{CO})_2$ species.^{13–15,24,25} These geminal species are thus *complex-specified*, and the reason for their formation is believed to be the reaching of a stable electron configuration.^{34,35} However, the low coordination of the Ir^+ cations permits formation of *site-specified* tri- and tetracarbonyls, i.e., species which lose stepwise their ligands under destruction.²⁶ On the basis of these observations and making analogy with other samples, for instance Co-ZSM-5,¹⁵ we can infer that the Ir^+ cations in Ir-

ZSM-5 that are able to form tetracarbonyls are located in cationic positions. Indeed, the observation that some of the zeolite acidic hydroxyls have been consumed after deposition of iridium proves the existence of exchanged iridium cations. Note also that Lefebvre et al.²⁰ using Ir-NaFAU and Ir-NaMOR samples prepared by wet ion exchange observed, after CO adsorption, bands at 2100 and 2080 cm^{-1} , which are similar to the bands of $\text{Ir}^+(\text{CO})_3$ species observed in this study.

The other kind of $\text{Ir}^+(\text{CO})_2$ species that we observed in this study was characterized by bands at 2127 and 2011 cm^{-1} . Through the use of the integral intensities of the carbonyl bands it can be roughly estimated that these cations amount to approximately one-fourth of all iridium cations in the sample. The respective carbonyls had stability comparable to that for the principal dicarbonyls of Ir^+ , which is consistent with the fact that the above complexes are stabilized by reaching stable electron configuration, this effect being much more important for the $\text{Ir}^+ - \text{CO}$ bond strength than the electrophilicity of the metal cation. It was found that these $\text{Ir}^+(\text{CO})_2$ species were not able to accommodate any additional CO molecule; i.e., the respective Ir^+ cations were more coordinatively saturated than the Ir^+ in cationic positions. Therefore, we stress that these iridium cations are not in exchange positions and behave rather as cations supported on oxides. Indeed, a series of system investigations have revealed that, as a rule, cations in zeolites are characterized by a lower coordination than the same cations supported on oxides.^{29,36,37} However, the possibility that these cations are affected by residual chlorine ions cannot be ruled out. In fact, solid-state ion exchange using metal chlorides has often been used as an effective alternative to prepare metal-exchanged zeolites (e.g., Fe-ZSM-5³⁸ and Co-ZSM-5³⁹), but in these cases residual chlorine ions can exist in the samples.

4.2. Other Carbonyl Complexes of Iridium in Ir-ZSM-5. In addition to the carbonyls of Ir^+ , we detected carbonyls of metallic iridium (2082–2060 cm^{-1}). These bands were observed with a higher intensity after activation procedure 2, which is consistent with the expected autoreduction of iridium at high temperatures. The $\text{Ir}^0 - \text{CO}$ bands will not be discussed here in more detail because they are beyond the scope of this study. We shall only note that bridging carbonyls were detected neither with metallic nor with cationic iridium. In fact, bridging CO is not typical for cations because of steric reasons: the large distance between the cations.³

The other new kind of nonclassical dicarbonyls that we report in this study are the $\text{Ir}^{2+}(\text{CO})_2$ species. The key treatment leading to their creation was sample evacuation at 673 K. At present we are not able to give a definite answer concerning the pathway of the appearance of these cations. Nevertheless we can propose three possible routes:

- The Ir^{2+} cations have existed on the sample after activation procedure 1 but have been coordinatively saturated. Evacuation at 673 K generates *cus* Ir^{2+} cations.
- The Ir^{2+} cations have been created via reduction of particular Ir^{3+} ions by CO desorbed at higher temperatures.
- The Ir^{2+} cations have been formed via oxidation of some Ir^+ cations as a result of CO dissociation. Indeed, although CO usually acts as a reducing agent, CO-induced oxidation of a surface site can occur as it is the case for Rh.²⁵

We can speculate that the Ir^{2+} cations forming dicarbonyls are in exchange positions in the zeolite, while the Ir^{2+} cations forming monocarbonyls only (band at 2159 cm^{-1}) have another location and are rather similar to cations supported on oxides.

Finally, we would like to emphasize that, to the best of our

knowledge, no $\text{Ir}^+(\text{CO})_4$ and $\text{Ir}^{2+}(\text{CO})_2$ polycarbonyls have been reported so far.

5. Conclusions

- Ir^+ cations in ZSM-5 can be highly coordinatively unsaturated being thus able to absorb up to four CO molecules each.
- Ir^{2+} cations in Ir-ZSM-5 form, upon CO adsorption, the unknown so far $\text{Ir}^{2+}(\text{CO})_2$ geminal dicarbonyls.

Acknowledgment. This work was supported by the Bulgarian National Research Foundation (Project No. X-1205) and the French–Bulgarian program RILA. E.I. is grateful to the French Ministry of Higher Education and Research for a one-year postdoctoral fellowship.

References and Notes

- (1) Aubke, F.; Wang, C. *Coord. Chem. Rev.* **1994**, *137*, 483.
- (2) Xu, Q. *Coord. Chem. Rev.* **2001**, *231*, 83.
- (3) Hadjiivanov, K.; Vayssilov, G. *Adv. Catal.* **2002**, *47*, 347.
- (4) Knözinger, H. In *Handbook of Heterogeneous Catalysis*; Ertl, G., Knözinger, H., Weitkamp, J., Eds.; Wiley–VCH: Weinheim, Germany, 1997; Vol. 2.
- (5) Davydov, A. *Molecular Spectroscopy of Oxide Catalyst Surfaces*; Wiley: Chichester, U. K., 2003.
- (6) Bordiga, S.; Escalona Platero, E.; Otero Arean, C.; Lamberti, C.; Zecchina, A. *J. Catal.* **1992**, *137*, 179.
- (7) Hadjiivanov, K.; Knözinger, H. *Chem. Phys. Lett.* **1999**, *303*, 513.
- (8) Hadjiivanov, K.; Knözinger, H.; Ivanova, E.; Dimitrov, L. *Phys. Chem. Chem. Phys.* **2001**, *3*, 2531.
- (9) Mihaylov, M.; Hadjiivanov, K.; Knözinger, H. *J. Phys. Chem. B* **2002**, *106*, 2218.
- (10) Chakarova, K.; Mihaylov, M.; Hadjiivanov, K. *Microporous Mesoporous Mater.* **2005**, *81*, 305.
- (11) Jang, S. B.; Jeong, M. S.; Kim, Y.; Song, S. H.; Seff, K. *Microporous Mesoporous Mater.* **1999**, *28*, 193.
- (12) Spoto, G.; Zecchina, A.; Bordiga, S.; Ricchiardi, S.; Martra, G.; Leofanti, G.; Petrini, G. *Appl. Catal., B* **1994**, *3*, 151.
- (13) Miessner, H.; Burkhardt, I.; Gutschick, D.; Zecchina, A.; Morterra, C.; Spoto, G. *J. Chem. Soc., Faraday Trans.* **1990**, *86*, 2321.
- (14) Ivanova, E.; Hadjiivanov, K. *Phys. Chem. Chem. Phys.* **2003**, *5*, 655.
- (15) Hadjiivanov, K.; Tsyntsarski, B.; Venkov, Tz.; Klissurski, D.; Daturi, M.; Saussey J.; Lavalley, J.-C. *Phys. Chem. Chem. Phys.* **2003**, *5*, 1695.
- (16) Iliopoulou, E.; Efthimiadis, E.; Nalbandian, L.; Vasalos, I.; Barth, J.; Lercher, J. A. *Appl. Catal., B* **2005**, *60*, 277.
- (17) Wisniewski, M.; Boréave, A.; Gélén, P. *Catal. Commun.* **2005**, *6*, 596.
- (18) Marzialelli, T.; Fierro, J. L. G.; Reyes, P. *Catal. Today* **2005**, *107–108*, 235.
- (19) Solymosi, F.; Novak, E.; Molnar, A. *J. Phys. Chem.* **1990**, *94*, 7250.
- (20) Lefebvre, F.; Auroux, A.; Ben Taarit, Y. *Stud. Surf. Sci. Catal.* **1985**, *24*, 411.
- (21) Gelin, P.; Goudurier, G.; Ben Taarit, Y.; Naccache, C. *J. Catal.* **1981**, *70*, 32.
- (22) Gelin, P.; Auroux, A.; Ben Taarit, Y.; Gravelle, P. *Appl. Catal.* **1989**, *46*, 227.
- (23) Bukhardt, I.; Gutschick, D.; Landmesser, H.; Miessner, H. In *Zeolite Chemistry and Catalysis*; Jacobs, P. A., Ed.; Elsevier: Amsterdam, 1991; p 215.
- (24) Ivanova, E.; Mihaylov, M.; Thibault-Starzyk, F.; Daturi, M.; Hadjiivanov, K. *J. Catal.* **2005**, *236*, 168.
- (25) Basu, P.; Panayotov, D.; Yates, J. T., Jr. *J. Am. Chem. Soc.* **1988**, *110*, 2074.
- (26) Hadjiivanov, K.; Ivanova, E.; Klissurski, D. *Catal. Today* **2001**, *70*, 75.
- (27) Nawdali, M.; Praliald, H.; Primet, M. *Top. Catal.* **2001**, *16–17*, 199.
- (28) Maache, M.; Janin, A.; Lavalley, J.-C.; Benazzi, E. *Zeolites* **1995**, *15*, 507.
- (29) Lynds, L. *Spectrochim. Acta* **1964**, *20*, 1369.
- (30) Hadjiivanov, K.; Kantcheva, M.; Klissurski, D. *J. Chem. Soc., Faraday Trans.* **1996**, *92*, 4595.
- (31) Bratermann, P. S. *Metal Carbonyl Spectra*; Academic Press: London, 1975.
- (32) Ripan, B.; Ceteanu, I. *Chemistry of Metals*; Mir: Moscow, 1972.
- (33) Rice, M. J.; Chakraborty, A. K.; Bell, A. T. *J. Catal.* **2000**, *194*, 278.
- (34) Van't Blik, H. F. J.; van Zon, J. B. A. D.; Huizinga, T.; Vis, J. C.; Koningsberger, D. C.; Prins, R. *J. Am. Chem. Soc.* **1985**, *107*, 3139.
- (35) Goellner, J. F.; Gates, B. C.; Vayssilov, G. N.; Rösch, N. *J. Am. Chem. Soc.* **2000**, *122*, 8056.
- (36) Mihaylov, M.; Hadjiivanov, K. *Langmuir* **2002**, *18*, 4376.
- (37) Hadjiivanov, K.; Knözinger, H. *J. Phys. Chem. B* **1998**, *102*, 10936.
- (38) Chen, H.-Y.; Sachtler, W. M. H. *Catal. Today* **1998**, *42*, 73.
- (39) Wang, X.; Chen, H.-Y.; Sachtler, W. M. H. *Appl. Catal., B* **2000**, *26*, L227.